Laboratory Investigation

Stereotactic and Functional Neurosurgery

Stereotact Funct Neurosurg 2015;93:255–264
DOI: 10.1159/000380826

Received: September 25, 2014
Accepted after revision: February 10, 2015
Published online: June 6, 2015

A Neuroimaging Strategy for the Three-Dimensional in vivo Anatomical Visualization and Characterization of Insular Gyri

Allison Rosen[a] David Qixiang Chen[a] Dave J. Hayes[b, c] Karen D. Davis[a–c] Mojgan Hodaie[a–c]

[a]Institute of Medical Science and Department of Surgery, University of Toronto, [b]Division of Brain, Imaging and Behaviour – Systems Neuroscience, Toronto Western Research Institute, University Health Network, and [c]Division of Neurosurgery, Department of Surgery, Toronto Western Hospital, Toronto, Ont., Canada

Key Words

Freesurfer · Gyrus · Human · Insula · Laterality · Magnetic resonance imaging · Neuroanatomy · Sex difference · Sulcus

Abstract

Background: Interest in the anatomy of the insula is driven by its multifunctionality and the need for accurate visualization for surgical purposes. Few in vivo studies of human insular anatomy have been conducted due to methodological and anatomical challenges. ***Objective:*** We used brain cortical morphometry tools to accurately reconstruct insular topology and permit a detailed visualization of its gyri in 3 dimensions. ***Methods:*** Sixty healthy subjects (33 females; 37.8 ± 12.8 years) underwent 3-tesla MRI scans. The strategy for characterizing the insula was: (1) create 3-dimensional (3-D) insula representations for visual analysis; (2) rate topological features using a gyral conspicuity index; (3) identify individual variations across subjects/between groups; (4) compare to prior findings. ***Results:*** Insular reconstruction was achieved in 113/120 cases. The anterior short, posterior short, anterior long gyri and central sulcus were easily identified. In contrast, middle short (MSG), posterior long (PLG) and accessory gyri (AG) were highly variable. The MSG, but not the PLG or AG, was clearer in males and in the left hemisphere, suggesting sex- and laterality-related differences. ***Conclusions:*** A noninvasive in vivo 3-D visualization strategy revealed anatomical variations of the insula in a healthy cohort. This methodological approach can be adopted for broad clinical and/or research purposes.

Introduction

The human insula is an anatomically and functionally complex structure located deep within the lateral sulcus, or sylvian fissure, and concealed by the opercula [1–5]. Over 200 years have passed since Reil first described the insula in detail [6], yet few detailed in vivo studies of its anatomy exist due partly to the methodological difficulties in imaging the opercular cortex. The cytoarchitectonic organization of the primate insula consists of 3 concentric agranular, dysgranular and granular zones [7–9], although their relation to the broader morphology is still unclear [8]. The earliest in vivo studies by Talairach in 1967, Szikla in 1977 and later Steinmetz and colleagues in 1989 used techniques such as pneumoencephalography, angiography and structural MRI, respectively, to help

Allison Rosen, David Qixiang Chen and Dave J. Hayes contributed equally to this work.

1011–6125/15/0934–0255$39.50/0

E-Mail karger@karger.com
www.karger.com/sfn

Mojgan Hodaie
Division of Neurosurgery, Toronto Western Hospital
399 Bathurst Street
Toronto, ON M5T 2S8 (Canada)
E-Mail mojgan.hodaie@uhn.on.ca

identify lateralized morphological differences such as greater left-side length of the lateral sulcus and size of the operculum [10].

In contrast to the in vivo anatomical data, there is substantial literature on the function of the insula in the healthy and diseased state [11–14]. Its widespread intra- and interstructural connections [5, 15] are in line with its role in many neural processes, for instance related to autonomic control and interoception [16–18], gustation [19, 20] somatosensation and pain [5, 21–24] and valuation [14, 25]. Mapping studies support a strong correlation between insular function and anatomy [26–28]. For example, stimulation experiments in those with epilepsy have correlated viscero- and somatosensory functions to the anterior and posterior insular regions, respectively [29]. Such findings support a relationship between gross anatomy and function at the subregional level.

Postmortem studies on the insula have examined its position relative to the overlying opercula or central sulcus [30], the lengths of insular gyri [31] or the vasculature running over the insula [3], but few studies have characterized detailed anatomical features of the insula itself. Nonetheless, they have converged upon a standard insular nomenclature whereby the insula is delineated by the peri-insular sulci (anterior, superior, posterior and inferior) and divided by the central insular sulcus (CIS) into anterior and posterior regions [3, 4, 30–33]. Variations in insular anatomy across individuals have been noted, as well as group differences including an increased number of gyri in the left compared to the right hemisphere [34] and in males compared to females [4, 33]. Most studies report the presence of 5 major gyri including the anterior short (ASG), middle short (MSG) and the posterior short gyri (PSG) of the anterior insula, and the anterior long (ALG) and posterior long gyri (PLG) of the posterior insula. Another commonly noted, but somewhat less identified, gyrus in the anterior insula includes the accessory gyrus (AG).

Few studies have used MRI to explore the anatomy of the insula. The first of such studies successfully outlined the rough 3-dimensional (3-D) topology of a single human insula using serial axial MR slices on a 1.0-tesla scanner, without revealing much anatomical detail [35]. Primarily due to technological advancements (e.g. increased magnetic field strength and more powerful computing), later studies contributed to this literature by demonstrating a coherence between gross anatomy and MR images from both indirect [4, 33] and direct comparisons [8] – using visual comparisons in the former and the coregistration of postmortem and MR slices in the latter. Such advancements have allowed for more nuanced in vivo analysis, akin to that noted in postmortem studies, and have also paved the way for the development of more advanced 2-D and 3-D reconstructions of the insula for improved visualization and analysis [36, 37]. Despite these advancements, there exists a need for standardized strategies towards the visualization and analysis of insular morphology for use particularly in a clinical setting.

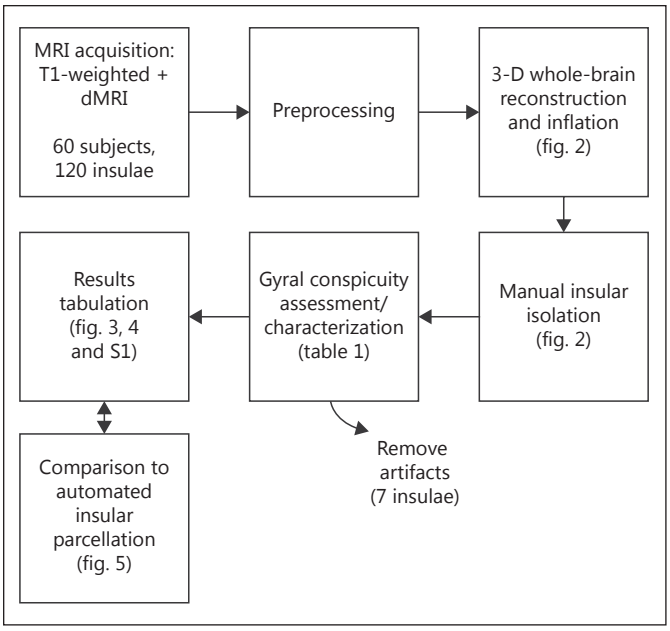

Fig. 1. Strategy for assessment of insular anatomy. An outline of the pipeline for the acquisition, analysis and visual characterization of individual insular anatomy. dMRI = Diffusion magnetic resonance imaging.

The aim of the current study was to develop a strategy for noninvasive, in vivo, neuroimaging of the insula and to investigate the feasibility of this approach to assess insular anatomy. Our specific goals were to (a) produce an accurate 3-D reconstruction of insular anatomy, (b) visualize precise gyral/sulcal insular anatomy and (c) assess variations in the normal anatomy of the insula, including sex and laterality differences.

Materials and Methods

The steps outlining the methodological strategy involved in the reconstruction, visualization, and assessment of the insulae are illustrated in figure 1.

Subjects and Image Acquisition

Sixty healthy right-handed volunteers (33 female, 27 male; mean age = 37.8 ± 12.8 years) with no history of known neuro-

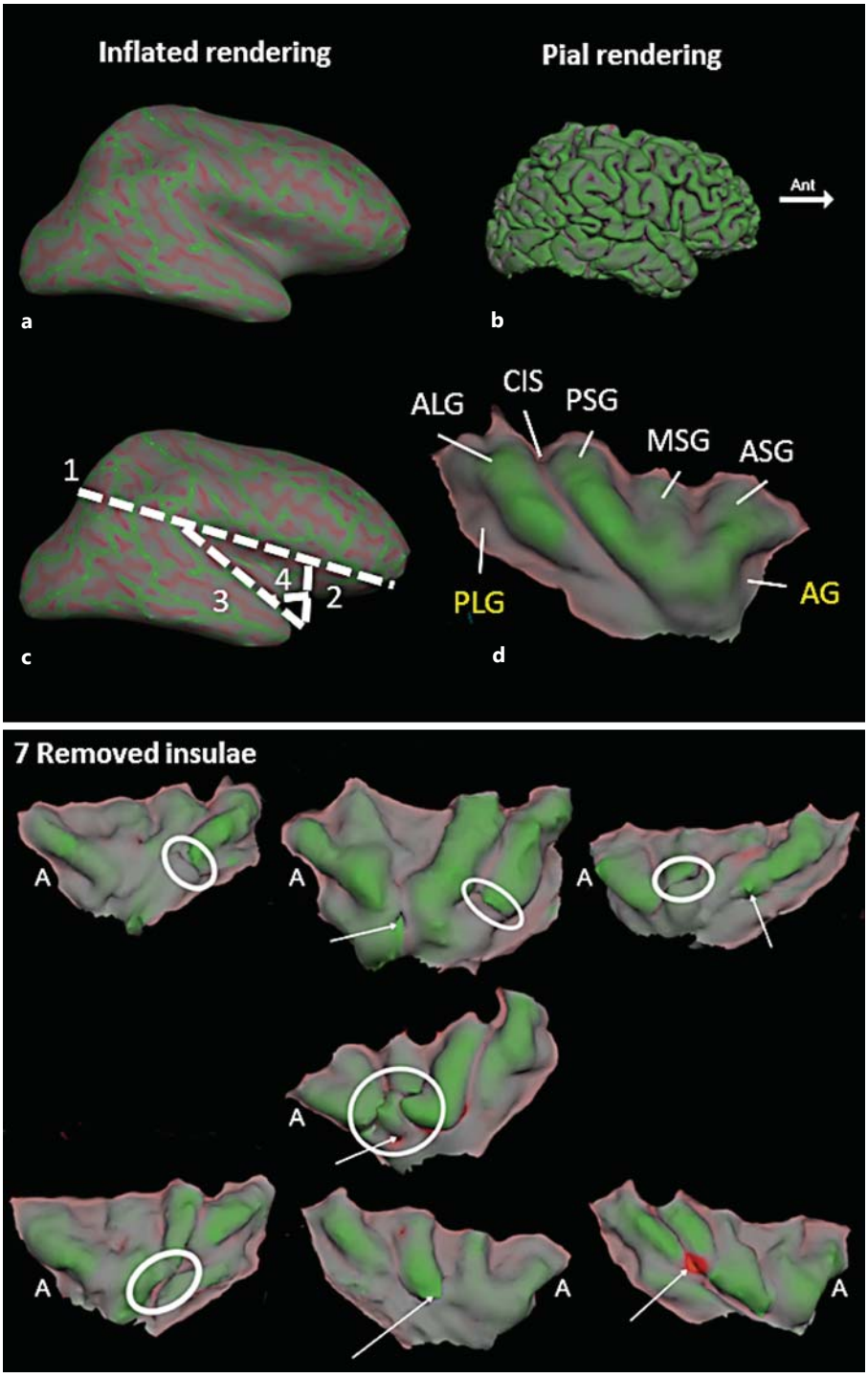

Fig. 2. Manual isolation and topology of a single insula (top panel) and 7 insulae removed for anomalies (bottom panel). **Top panel:** Isolation of a sample insula from a right hemisphere is shown. **a** Inflated renderings. **b** Pial renderings. **c** Isolation of the insula using 4 cut lines, in order of cutting. **d** The final isolated insula in the pial rendering. In this example, of the 6 major insular gyri investigated, 4 can be seen clearly (ASG, MSG, PSG, ALG noted in white text) and 2 cannot (AG, PLG noted in yellow text). The central insular sulcus (CIS) is also clearly visible. Red indicates sulci, and green indicates gyri. **Bottom panel:** Abnormal gyral truncations (encircled) or abrupt/uneven changes in curvature (arrowed) were the criteria by which insular reconstruction was considered incomplete/incorrect. A = Anterior.

logical or psychiatric disorders had been recruited to participate in the study. Informed consent was obtained from each subject for procedures approved by the University Health Network Research Ethics Board. Each subject had a high-resolution MRI in a 3-tesla General Electric scanner (GE Medical Systems, Milwaukee, Wis., USA) with an 8-channel head coil. T1-weighted anatomical images were acquired with an axial fast spoiled gradient (FSPGR) sequence, slice thickness = 1 mm, number of slices = 124, repetition time = 25 ms, echo time = 5 ms, 45° flip angle, matrix = 256 × 256, field of view = 24 cm.

Image Processing and 3-D Rendering

T1-weighted images were analyzed using Freesurfer software found at http://surfer.nmr.mgh.harvard.edu [38–41]. The pipeline

Table 1. Conspicuity criteria

Area	Rating key	Visualization
All gyri	3	clear
	2	unclear
	1	unseen
	single	single gyrus
	bifid	gyrus bifurcatus
CIS	4	clear (continuous)
	3	clear (discontinuous)
	2	unclear
	1	unseen
AG	3	clear
	2	unclear
	1	unseen
MSG	yes	hypoplastic
	no	not hypoplastic
PLG	separate	clearly demarcated from the ALG by a postcentral insular sulcus, even if that sulcus is hypoplastic
	branched	appeared to represent a short segment arising from the posteroinferior aspect of the ALG

Top: criteria used for all gyri; bottom: additional criteria used for specific anatomy.

included normalization of image intensity, skull stripping of images, separation of the hemispheres, segmentation of gray matter and delineation of CSF-gray matter (pial surface) and gray matter-white matter (white surface) boundaries. This approach was used given prior cortical reconstruction validations in both postmortem and in vivo samples [38, 42, 43]. Processed MRI scans were viewed using TkSurfer, a program within Freesurfer. The resulting 3-D pial surface rendering of a single hemisphere was examined in an inflated view, to expose an unobstructed view of the insula. The inflated viewing modality lifts temporal, parietal and frontal opercula that normally cover the insula, and provides visualization of the entire hemisphere as a smoothed surface. Curvature overlay views were applied to the cortical surface, indicating positive (sulci) and negative (gyri) curvature values at each point on the hemisphere in red and green, respectively [44]. This facilitated an accurate anatomical localization of the insula. To view the insula in isolation, we used the TkSurfer-inflated renderings and manually removed all noninsular areas in a stepwise fashion (fig. 2).

Four initial boundary definitions were made, and cuts were made in the following order: (1) structures superior to the insula, as described above; (2) anterior structures; (3) posterior structures; (4) inferior structures, which involved cutting along the inferior apex of the insula in a short anterior-to-superior line (fig. 2c). The insula was then returned to a pial rendering where cortical topology of the insula could be clearly visualized (fig. 2d).

Once isolated, we inspected all images to ensure that they contained the insula and no other anatomical structures by visualizing each hemisphere as a pial rendering and examining the gyral contours. Confirmation of reconstructed insular anatomy was made using postmortem and prior MR atlases [3, 36]. This helped identify possible remnants from the medial surface of the hemisphere, such as the anterior cingulate cortex, which were manually removed. A rendering was considered complete when the insula was viewed in isolation and unobstructed by surrounding structures. Insular reconstructions were rejected if major topological errors were present, such as discontinuous gyri or uneven cortical surfaces.

Characterization of Gyri

Whether each reconstructed gyrus or sulcus is present or absent, when viewed in the pial rendering, is determined using visualization or conspicuity criteria (table 1). However, we noted instances where structures were not identified fully along their predicted axes – e.g. the gyrus may appear to split or terminate sooner than expected. As such, the visualization of gyri and sulci was rated using an assessment of conspicuity to distinguish between such instances. The 6 main gyri (ASG, MSG, PSG, ALG, PLG and AG) and CIS were each assessed and identified as 'unseen', 'unclear' or 'clear'.

Four main criteria were considered when identifying the conspicuity of a gyrus: (1) clarity of sulcal boundaries; (2) margins throughout the course of the gyrus; (3) apparent prominence and ease of viewing the gyrus, and (4) the color of the curvature overlay on the gyrus. Additional topological anomalies such as bifidity (splitting of the gyrus) or apparent hypoplasia (underdevelopment) of the gyri were noted. Hypoplasia of the MSG was noted if the gyrus protruded laterally to a lesser degree than the neighboring ASG and PSG, as determined by a decreased relative color intensity (representing a smaller gyral contour) using the curvature overlay. The PLG was rated as either separate, where it was demarcated from the ALG by a postcentral insular sulcus, or branched, in which case the ALG represented only a short segment associated with the posteroinferior aspect of the ALG.

Following the visual identification of apparent differences in subregional topology, nonparametric statistical tests were carried out. These included the Wilcoxon signed-rank test for within-subject (i.e. lateralized differences between left and right subregions) comparisons and the Mann-Whitney test for between-subject (i.e. males vs. females) comparisons.

Finally, we compared our method of direct insular examination to the automated anatomical parcellation provided by Freesurfer. This parcellation does not include a precise localization of each gyrus and the CIS, but instead provides an 'inner' outline of each group of short and long gyri as well as the 'outer' boundaries (i.e. the limiting sulci) of the insula. We pseudorandomly selected one third of our sample (i.e. 37 insulae; excluding those with more than 2 structures labeled 'unseen') to compare key anatomical features as derived by individual examination and automated parcellation.

Results

Topological 3-D Reproductions of the Insula Yield Anatomically Accurate Images

To determine whether our technique was able to accurately reproduce 3-D representations of the cortical sur-

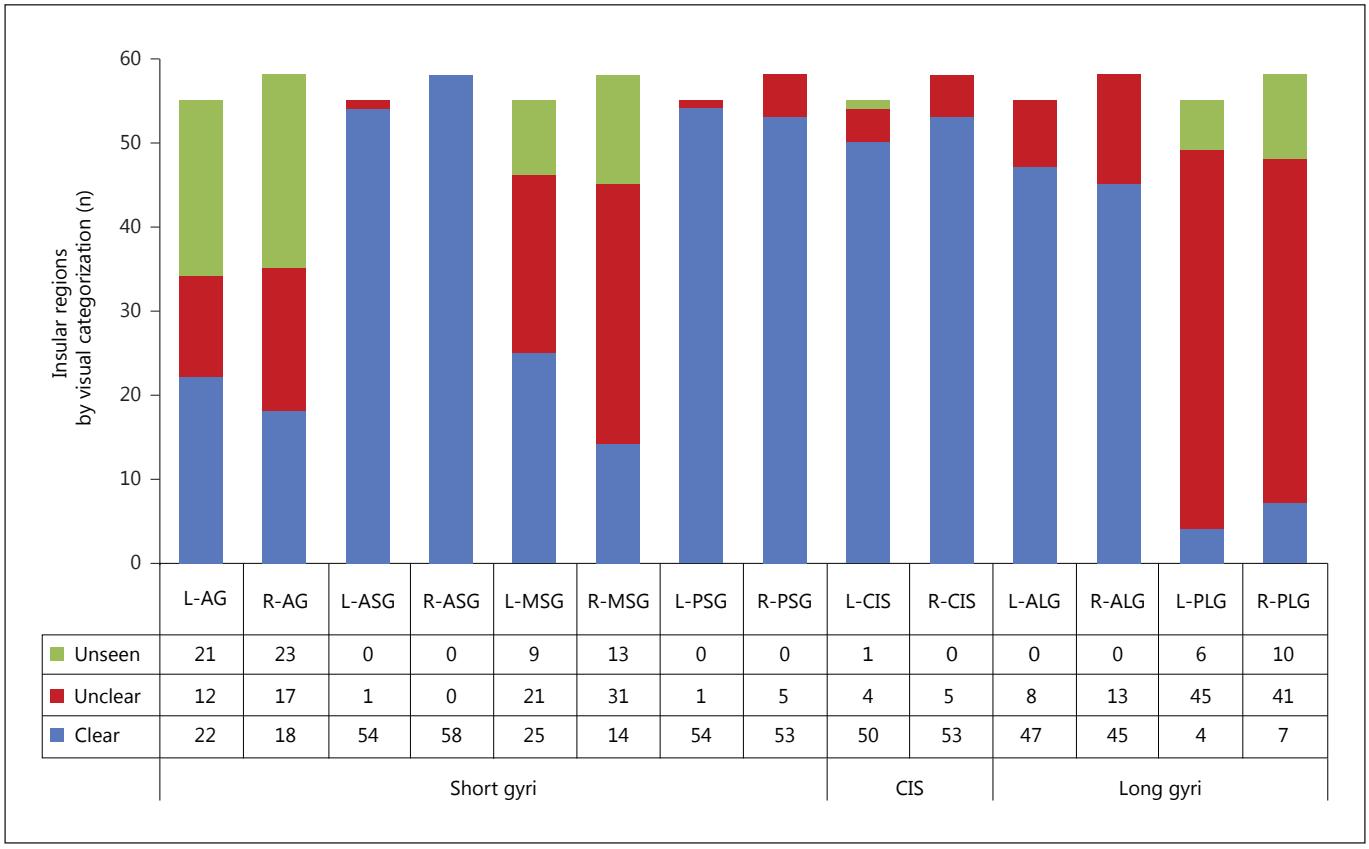

	L-AG	R-AG	L-ASG	R-ASG	L-MSG	R-MSG	L-PSG	R-PSG	L-CIS	R-CIS	L-ALG	R-ALG	L-PLG	R-PLG
Unseen	21	23	0	0	9	13	0	0	1	0	0	0	6	10
Unclear	12	17	1	0	21	31	1	5	4	5	8	13	45	41
Clear	22	18	54	58	25	14	54	53	50	53	47	45	4	7
	Short gyri								CIS		Long gyri			

Fig. 3. Visual characterization of insular anatomy shows subregional variability. The distribution of visualization ratings among the 3 categories ('clear' in blue; 'unclear' in red; 'unseen' in green) is divided by side of the brain (L = left; R = right).

face of the insula, we first examined all 120 reconstructions for possible errors guided by standard postmortem determined topology [3]: 113 out of 120 reconstructions (94%) showed anatomically reliable representations of the insula. The major topological features observed in any single subject revealed an insular cortex that was free of interruptions in the cortical topology, such as sudden gyral truncations or cortical thickness anomalies, as represented by intensity of red/green curvature maps (fig. 2). Reconstructions containing such distortions were excluded from subsequent structural analyses (n = 7; fig. 2). Topological errors and sudden gyral truncations were easily observed in the excluded images but were absent in the rest of the sample, which looked like the example in figure 2.

Variations in Insular Anatomy

Visual Characterization of Gyri and Central Sulcus across Subjects

Differing degrees of variability were noted across insular gyral subregions. The ASG, PSG, ALG as well as the CIS showed high levels of consistency and visibility across individuals, while other gyri, such as the AG, MSG and PLG were more variable and often difficult to identify (fig. 3). We used additional visualization assessments to note the degree of anatomical variation of the individual insular gyri (table 1). ASG, PSG and ALG were all 'clear' in over 80% of insulae, while AG, MSG and PLG contained the greatest amount of anatomical variation and were either 'unclear' or 'unseen' in over 65% of insulae. Also, the majority of gyri were nonbifurcated, while the highest rates of bifid gyri were noted in the generally largest and broadest insular structures of the ASG (35%) and ALG (27%) (online suppl. table S1; for all online suppl. material, see www.karger.com/doi/10.1159/000380826).

Of the 97 (out of 113) observed PLG, 66% were branched off from the ALG, while 34% were distinctly separate from the ALG. Branched PLG were visually differentiated from bifid ALG by point of branching. Branched PLG began at a more ventral aspect of the ALG, while ALG were observed to bifurcate starting from a

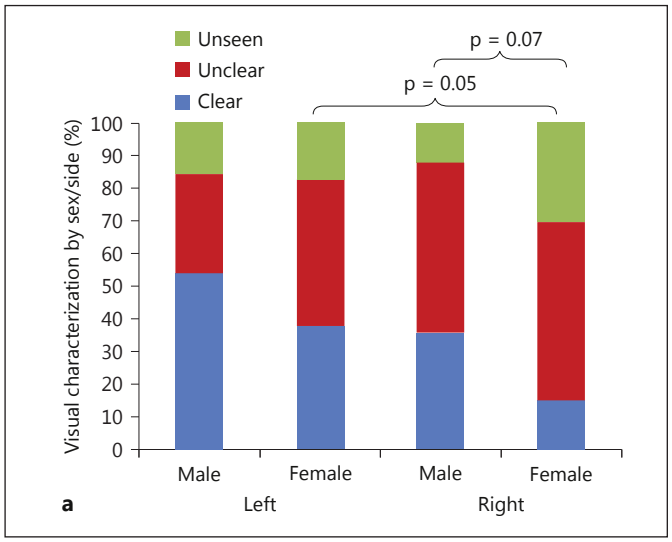

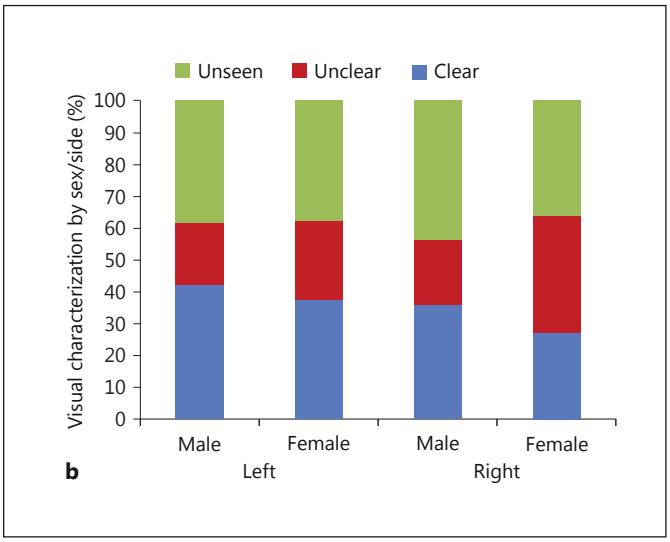

Color version available online

Fig. 4. Visual characterization of MSG and AG by side and sex; 'clear' in blue; 'unclear' in red; 'unseen' in green; L = left; R = right. Note that given a nonequal number of male and female insulae, the results are displayed as percent visual characterization ratings divided by side of the brain as opposed to figure 3 which shows the number of regions identified. **a** Percent visualization ratings for the MSG among the 3 categories. **b** Percent visualization ratings for the AG among the 3 categories.

more dorsal aspect of the gyrus. It is noted that all PLG appeared less prominent in relation to the adjacent ALG. The MSG was observed in 81% of the examined insulae, and appeared less prominent relative to adjacent gyri in 55% of the cases. The PSG and CIS appeared to be the most consistent structures in the insula, as they were rated 'clear' in 95 and 91% of cases, respectively, with the CIS being fully continuous in 83% (i.e. in 86 of 103 of those labeled 'clear'). Only 1 insula contained no observable CIS (fig. 2). The AG could be recognized by its characteristic truncation at a level more ventral to that of the other short insular gyri. Visualization of the AG was highly variable, ranging from 'unseen' (39%) to 'unclear' (25%) and 'clear' (36%).

A Closer Look at MSG and AG Variability

Given the visually apparent sex- and laterality-related differences, as noted in figure 3 and online supplementary figure S1, further nonparametric statistical analyses were carried out within the MSG and AG subregions (fig. 4a, b). The PLG was not considered further given the especially low percentage of 'clear' ratings.

For the MSG (fig. 4a), the Wilcoxon signed-rank test, used to identify within-group differences, showed that the visibility of male MSG was similar between sides ($Z = -1.508$, $p = 0.132$) while female right MSG were more difficult to identify clearly ($Z = -1.964$, $p = 0.05$). The Mann-Whitney test for between-group comparisons showed no difference of the left ($U = 297$, $Z = -1.250$, $p = 0.221$) or right ($U = 267$, $Z = -1.840$, $p = 0.066$) MSG between sexes, although there was a trend toward decreased characterization of the right female MSG compared to the male – which is consistent with the difference noted within female participants alone.

For the AG (fig. 4b), the Wilcoxon signed-rank test showed that the visibility of male ($Z = -0.722$, $p = 0.470$) and female ($Z = -0.431$, $p = 0.666$) MSG was similar between sides. The Mann-Whitney test for between-group comparisons showed no difference of the left ($U = 345$, $Z = -0.335$, $p = 0.738$) or right ($U = 360$, $Z = -0.055$, $p = 0.956$) AG between sexes.

Atlas Comparison

To compare the described method with the automated Freesurfer atlas, we visualized the major boundaries of the insula as determined by our strategy with those calculated by the automated anatomical parcellation method in Freesurfer. Manual identification was generally superior to automated parcellation, as the latter was only able to outline the boundaries of the outer limiting sulci and the inner short and long gyri. However, both methods were able to clearly identify the CIS, and we observed a near-exact positional match in 35 out of 37 cases, with minor variation in the remaining 2. In contrast, the auto-

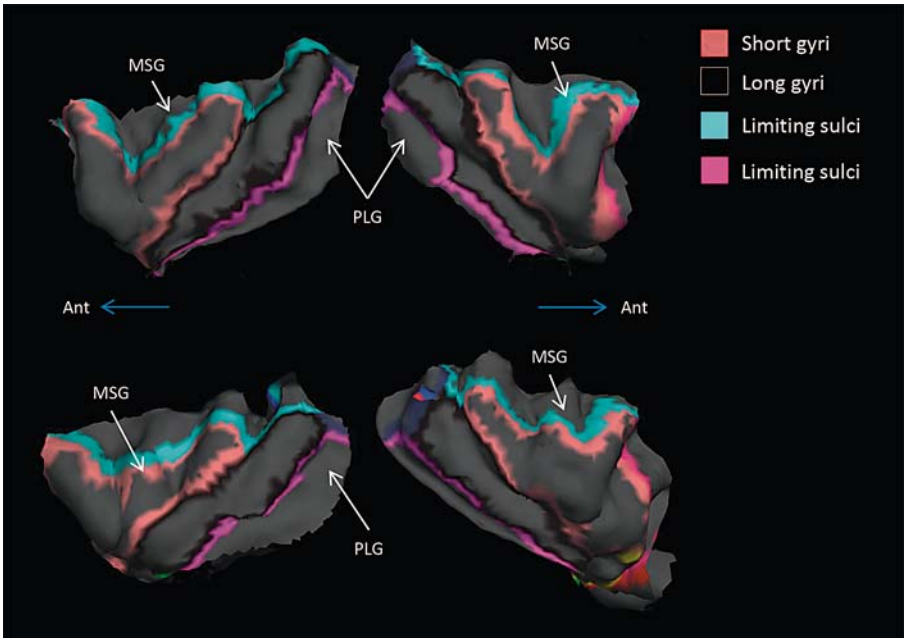

Fig. 5. Automated parcellation of insular topology is inferior to manual identification. Sample automated insular parcellations show inconsistent identification of subregions. However, identification of the CIS (the line between black and peach) is highly consistent. The MSG is cropped in all test cases – i.e. not included in the outline of short gyri (peach color) and excluded by the limiting sulcus border (light blue color). The PLG is also cropped in all cases – i.e. not included in the outline of long gyri (black) and excluded by the limiting sulcus (pink).

mated atlas was found to mislabel MSG and PLG as limiting sulci in all 37 cases. Typical examples can be seen in figure 5.

Discussion

The present strategy used for this study demonstrated that: (1) a noninvasive 3-D reconstruction of the insula is feasible and comparable to invasive techniques, such as postmortem studies; (2) a visualization strategy can accurately outline the features of an individual insula and help identify variability in the gyri. Going forward, the accurate identification of variability across insular subregions will be of significant importance for neurosurgical planning, and for clinical research focused on insular structure and function. This is emphasized by findings that conspicuity may be linked to differences in overall surface area [44] and by reiterating that the insula's polymodal functions are strongly linked to differential insular subdivisions [7, 26, 27]. The strategy presented here, which outlines a pipeline for the accurate 3-D reconstruction, visual assessment and characterization of insular topology, is a significant improvement on current strategies – ranging from the simple inspection of MR images in a neurosurgical context [4] to the highly technically complex analysis employed in some neuroscience experiments [8], which may be less feasible for use in neurosurgical or clinical studies.

In vivo Visualization of Insular Features across Individuals

Although gyral variation has not previously been examined in this level of detail in vivo, we explored previous studies in this field to determine any similarities or differences in description of the gyri. These comparisons are important in validating our strategy and help establish it as a useful strategy when compared with direct anatomical assessments of the insula. Accordingly, we observed that the CIS was clearly seen in 91% of cases, similar to other studies where the CIS was easily identified in 90 and 95% of cases [30, 31]. Further, we observed increased variability in the anterior lobe of the insula, with the more variable gyrus being the MSG, as is consistent with prior findings [4, 31, 33, 34]. Although broadly consistent with prior literature, our approach revealed subtle similarities and differences in insular morphology across individuals which should be considered by investigators in this area.

Visual assessment revealed that some of the insular gyri (ALG, ASG and PSG) are consistently observed while others (AG, MSG and PLG) have a much higher degree of structural variability. We observed laterality and a trend toward sex-related differences in the MSG, with a tendency toward increased visibility on the left side in

males. Interestingly, various studies of emotion, pain and self-awareness have reported relevant functional laterality differences, although these reports have thus far been unable to pinpoint specific gyri [11, 23, 45, 46]. The highly variable MSG is a region known for having viscerosensory and gustatory sensory roles, giving rise to the question of whether the integration of these functions shows corresponding variability across individuals. This is of particular interest when considering the role of the insula in more integrative functions such as interoception [16, 47], affective-sensory pain signaling [21, 45] and gustatory processing [47]. Although no studies have yet investigated laterality- or sex-related differences in the MSG, 2 human studies using direct electrical stimulation have identified this region bilaterally in the production of speech and the sensory component of pain [48, 49].

The high variability of other structures, the AG and PLG, did not appear clearly related to sex or laterality differences in our sample. For instance, variability of the PLG may be due to differences in its separation from the ALG, where most 'clear' PLG (34%) were separate from the ALG instead of branching off it. The AG variability has been reported elsewhere as being well developed (48%), underdeveloped (34%) or absent (18%) in a sample of 25 healthy postmortem brains [30], which is generally consistent with our findings. This proportion differs slightly from our study, however, where we see a much larger number of instances where the AG is absent in nearly 40% of cases (fig. 4b). Additionally, the dorsal border of the AG in our study consistently did not extend as far as the adjacent short gyri (see fig. 2 for reference). The reason for the differences between our study and the postmortem study is unclear but may be due to random sampling of a small number of subjects in the postmortem study and/or the ex vivo procedures involved, such as the preservation of brains over a 2-month period before investigation.

Other regions were relatively anatomically stable, such as the ASG and ALG regions, which are associated with gustation/interoception and somatosensory/gustation/thermosensory functions, respectively [50–53]. Although little else has been reported on the structural-functional relationships of these gyri, the ability to easily identify them should be conducive to an improved understanding of their structural-functional significance in future studies. The presently proposed strategy involving the noninvasive in vivo structural study of the insula is intended to help bridge this gap in current knowledge by providing a path for more detailed analysis correlating the structure of the subregional insula with function.

Automated Parcellation Does Not Allow for Insular Subregional Identification

A comparison of segmentation of insular structures with the automated Freesurfer atlas and our approach revealed that the position of the CIS in both techniques was identical in 95% of cases (see fig. 5 for examples). However, the more variable structures of the MSG and PLG were mislabeled by the Freesurfer atlas as the limiting sulcus or opercula in all instances. In practical terms, this implies that the Freesurfer atlas is useful for the study of the insula where a simple anterior-posterior division is preferred, as the atlas is highly unlikely to erroneously delineate the position of the CIS. However, where a more nuanced investigation of the insula's topology is required, we recommend the use of the presently proposed strategy, involving the direct visual inspection and assessment of an individual 3-D reconstructed insula. We suspect that the limitation in automatically identifying the MSG and PLG may be, at least partly, due to their relative flatness when compared to surrounding subregions – as this is computationally challenging using automated strategies [54].

Taken together, compared to existing automated strategies, the present improvements allow for two main benefits. First, the combination of accurate noninvasive imaging and improved characterization of insular subregions will allow for a greater understanding of possible structural variability, and their implications, across a range of clinical conditions in which altered insular structure and/or function is implicated. Moreover, these findings will provide an appreciation of the likelihood of subregional variability in healthy controls, and thus help prevent erroneous assumptions, and false positives, when assessing these insular areas in the context of disease.

Limitations and Conclusion

The identification of a so-called 'normal' insular topology was performed accurately and practically in the present study (fig. 2, 3). The major topological features observed in any single subject revealed an insular cortex that was free of interruptions in the cortical topology, such as sudden gyral truncations or cortical thickness anomalies, as represented by intensity of red/green curvature maps. However, the main limitation is that we are unable to know whether our excluded samples (n = 7) were the result of an abnormal insula in otherwise healthy people and/or whether the 3-D reconstructions produced errors related to some technical failures (e.g. an undefined error during processing with Freesurfer or subtle undetected artifacts in the native MR images) – although duplicate

analyses produced similar issues in these samples. As such, although we believe this strategy to be highly efficacious in most cases, we acknowledge that the investigation of some insular samples will require the standard visualization of MR images without using 3-D reconstructions. Importantly, the identification of abnormal insular structures, at least as identified through 3-D reconstruction, was visually obvious (fig. 2).

In conclusion, a better understanding of intra- and interindividual differences in the structure and function of the insula would aid greatly in the fields of neurosurgery and clinical neuroscience. For instance, minor variations in insular subregions may be both of structural and functional significance, as suggested by gyral differences associated with sex and laterality which have been the subject of attention in recent years and the focus of multiple ideas on the lateralization and polymodal functions of the insula [46]. These ideas can be explored more easily using the noninvasive strategy described here, with the hopes of eventually leading to an increased understanding of the physiological basis of some of these differences.

References

1 Fischl B, Stevens AA, Rajendran N, Yeo BTT, Greve DN, Van Leemput K, et al: Predicting the location of entorhinal cortex from MRI. Neuroimage 2009;47:8–17.
2 Fischl B, Rajendran N, Busa E, Augustinack J, Hinds O, Yeo BTT, et al: Cortical folding patterns and predicting cytoarchitecture. Cereb Cortex 2008;18:1973–1980.
3 Tanriover N, Rhoton AL, Kawashima M, Ulm AJ, Yasuda A: Microsurgical anatomy of the insula and the sylvian fissure. J Neurosurg 2004;100:891–922.
4 Mavridis I, Boviatsis E, Anagnostopoulou S: Exploring the neurosurgical anatomy of the human insula: a combined and comparative anatomic-radiologic study. Surg Radiol Anat 2011;33:319–328.
5 Augustine JR: Circuitry and functional aspects of the insular lobe in primates including humans. Brain Res Brain Res Rev 1996;22:229–244.
6 Fusar-Poli P, Howes O, Borgwardt S: Johann Cristian Reil on the 200th anniversary of the first description of the insula (1809). J Neurol Neurosurg Psychiatry 2009;80:1409.
7 Nieuwenhuys R: The insular cortex: a review. Prog Brain Res 2012;195:123–163.
8 Morel A, Gallay MN, Baechler A, Wyss M, Gallay DS: The human insula: architectonic organization and postmortem MRI registration. Neuroscience 2013;236:117–135.
9 Mesulam MM, Mufson EJ: The insula of Reil in man and monkey. Architectonics, connectivity, and function; in Peters A, Jones E (eds): Cerebral Cortex. New York, Plenum Publishing Corporation, 1985, pp 179–224.
10 Ochiai T, Grimault S, Scavarda D, Roch G, Hori T, Rivière D, et al: Sulcal pattern and morphology of the superior temporal sulcus. Neuroimage 2004;22:706–719.
11 Karnath H-O, Baier B: Right insula for our sense of limb ownership and self-awareness of actions. Brain Struct Funct 2010;214:411–417.
12 Ackermann H, Riecker A: The contribution(s) of the insula to speech production: a review of the clinical and functional imaging literature. Brain Struct Funct 2010;214:419–433.
13 Borsook D, Moulton EA, Pendse G, Morris S, Cole SH, Aiello-Lammens M, et al: Comparison of evoked vs spontaneous tics in a patient with trigeminal neuralgia (tic douloureux). Mol Pain 2007;3:34.
14 Lamm C, Singer T: The role of anterior insular cortex in social emotions. Brain Struct Funct 2010;214:579–591.
15 Mesulam MM, Mufson EJ: Insula of the old world monkey. I. Architectonics in the insulo-orbito-temporal component of the paralimbic brain. J Comp Neurol 1982;212:1–22.
16 Critchley HD, Wiens S, Rotshtein P, Ohman A, Dolan RJ: Neural systems supporting interoceptive awareness. Nat Neurosci 2004;7:189–195.
17 Craig AD: How do you feel? Interoception: the sense of the physiological condition of the body. Nat Rev Neurosci 2002;3:655–666.
18 Oppenheimer SM, Gelb A, Girvin JP, Hachinski VC: Cardiovascular effects of human insular cortex stimulation. Neurology 1992;42:1727–1732.
19 Mayer EA, Naliboff BD, Craig ADB: Neuroimaging of the brain-gut axis: from basic understanding to treatment of functional GI disorders. Gastroenterology 2006;131:1925–1942.
20 Roper SN, Lévesque MF, Sutherling WW, Engel J: Surgical treatment of partial epilepsy arising from the insular cortex. Report of two cases. J Neurosurg 1993;79:266–269.
21 Moayedi M, Weissman-Fogel I: Is the insula the 'how much' intensity coder? J Neurophysiol 2009;102:1345–1347.
22 Frot M, Magnin M, Mauguière F, Garcia-Larrea L: Human SII and posterior insula differently encode thermal laser stimuli. Cereb Cortex 2007;17:610–620.
23 Peltz E, Seifert F, DeCol R, Dörfler A, Schwab S, Maihöfner C: Functional connectivity of the human insular cortex during noxious and innocuous thermal stimulation. Neuroimage 2011;54:1324–1335.
24 Maihöfner C, Seifert F, Decol R: Activation of central sympathetic networks during innocuous and noxious somatosensory stimulation. Neuroimage 2011;55:216–224.
25 Hayes DJ, Duncan N, Xu J, Northoff G: A comparison of neural responses to appetitive and aversive stimuli in humans and other mammals. Neurosci Biobehav Rev 2014;45:350–368.
26 Kurth F, Zilles K, Fox PT, Laird AR, Eickhoff SB: A link between the systems: functional differentiation and integration within the human insula revealed by meta-analysis. Brain Struct Funct 2010;214:519–534.
27 Kurth F, Eickhoff SB, Schleicher A, Hoemke L, Zilles K, Amunts K: Cytoarchitecture and probabilistic maps of the human posterior insular cortex. Cereb Cortex 2010;20:1448–1461.
28 Penfield W, Faulk ME: The insula – further observations on its function. Brain 1955;78:445–470.
29 Ostrowsky K, Isnard J, Ryvlin P, Guénot M, Fischer C, Mauguière F: Functional mapping of the insular cortex: clinical implication in temporal lobe epilepsy. Epilepsia 2000;41:681–686.
30 Türe U, Yaşargil DC, Al-Mefty O, Yaşargil MG: Topographic anatomy of the insular region. J Neurosurg 1999;90:720–733.
31 Afif A, Mertens P: Description of sulcal organization of the insular cortex. Surg Radiol Anat 2010;32:491–498.
32 Cunningham DJ: The sylvian fissure and the island of Reil in the primate brain. J Anat Physiol 1891;25:286–291.
33 Naidich TP, Kang E, Fatterpekar GM, Delman BN, Gultekin SH, Wolfe D, et al: The insula: anatomic study and MR imaging display at 1.5 T. AJNR Am J Neuroradiol 2004;25:222–232.
34 Varnavas GG, Grand W: The insular cortex: morphological and vascular anatomic characteristics. Neurosurgery 1999;44:127–128.
35 Nawata M: MR visualization of the insula. Magn Reson Med Sci 2003;2:141–144.

36 Afif A, Hoffmann D, Becq G, Guenot M, Magnin M, Mertens P: MRI-based definition of a stereotactic two-dimensional template of the human insula. Stereotact Funct Neurosurg 2009;87:385–394.
37 Afif A, Becq G, Mertens P: Definition of a stereotactic 3-dimensional magnetic resonance imaging template of the human insula. Neurosurgery 2013;72:35–46, discussion 46.
38 Dale AM, Fischl B, Sereno MI: Cortical surface-based analysis. I. Segmentation and surface reconstruction. Neuroimage 1999;9:179–194.
39 Fischl B, Sereno MI, Dale AM: Cortical surface-based analysis. II. Inflation, flattening, and a surface-based coordinate system. Neuroimage 1999;9:195–207.
40 Fischl B, Liu A, Dale AM: Automated manifold surgery: constructing geometrically accurate and topologically correct models of the human cerebral cortex. IEEE Trans Med Imaging 2001;20:70–80.
41 Fischl B, van der Kouwe A, Destrieux C, Halgren E, Ségonne F, Salat DH, et al: Automatically parcellating the human cerebral cortex. Cereb Cortex 2004;14:11–22.
42 Cardinale F, Chinnici G, Bramerio M, Mai R: Validation of FreeSurfer-estimated brain cortical thickness: comparison with histologic measurements. Neuroinformatics 2014;12:535–542.
43 Rosas H, Liu A, Hersch S, Glessner M: Regional and progressive thinning of the cortical ribbon in Huntington's disease. Neurology 2002;05886:695–701.
44 Pienaar R, Fischl B, Caviness V, Makris N, Grant PE: A methodology for analyzing curvature in the developing brain from preterm to adult. Int J Imaging Syst Technol 2008;18:42–68.
45 Starr CJ, Sawaki L, Wittenberg GF, Burdette JH, Oshiro Y, Quevedo AS, et al: Roles of the insular cortex in the modulation of pain: insights from brain lesions. J Neurosci 2009;29:2684–2694.
46 Craig ADB: The sentient self. Brain Struct Funct 2010;214:563–577.
47 Small DM: Taste representation in the human insula. Brain Struct Funct 2010;214:551–561.
48 Afif A, Minotti L, Kahane P, Hoffmann D: Middle short gyrus of the insula implicated in speech production: intracerebral electric stimulation of patients with epilepsy. Epilepsia 2010;51:206–213.
49 Afif A, Hoffmann D, Minotti L, Benabid AL, Kahane P: Middle short gyrus of the insula implicated in pain processing. Pain 2008;138:546–555.
50 Brooks JC, Tracey I: The insula: a multidimensional integration site for pain. Pain 2007;128:1–2.
51 Simmons WK, Avery J, Barcalow JC, Bodurka J, Drevets WC, Bellgowan P: Keeping the body in mind: insula functional organization and functional connectivity integrate interoceptive, exteroceptive, and emotional awareness. Hum Brain Mapp 2013;34:2944–2958.
52 Afif A, Minotti L, Kahane P, Hoffmann D: Anatomofunctional organization of the insular cortex: a study using intracerebral electrical stimulation in epileptic patients. Epilepsia 2010;51:2305–2315.
53 Nitschke JB, Dixon GE, Sarinopoulos I, Short SJ, Cohen JD, Smith EE, et al: Altering expectancy dampens neural response to aversive taste in primary taste cortex. Nat Neurosci 2006;9:435–442.
54 Gao Y, Corn B, Schifter D, Tannenbaum A: Multiscale 3D shape representation and segmentation with applications to hippocampal/caudate extraction from brain MRI. Med Image Anal 2012;16:374–385.